In-orbit performance of Herschel-HIFI[⋆]

P.R. Roelfsema,[1] F.P. Helmich[1], D. Teyssier[2], V. Ossenkopf[1,3], P. Morris[4], M. Olberg[1,5], R. Shipman[1], C. Risacher[1], M. Akyilmaz[3], R. Assendorp[1], I.M. Avruch[1,28], D. Beintema[1], N. Biver[27], A. Boogert[4], C. Borys[4], J. Braine[23,24], M. Caris[6], E. Caux[7,8], J. Cernicharo[16], O. Coeur-Joly[7,8], C. Comito[6], G. de Lange[1], B. Delforge[10], P. Dieleman[1], L. Dubbeldam[1], Th. de Graauw[18], K. Edwards[17], M. Fich[17], F. Flederus[1], C. Gal[3], A. di Giorgio[12], F. Herpin[23,24], D. R. Higgins[22], A. Hoac[4], R. Huisman[1], C. Jarchow[9], W. Jellema[1], A. de Jonge[1], D. Kester[1], T. Klein[6], J. Kooi[20], C. Kramer[3], W. Laauwen[1], B. Larsson[13], C. Leinz[6], S. Lord[4], A. Lorenzani[11], W. Luinge[1], A. Marston[2], J. Martín-Pintado[16], C. McCoey[17], M. Melchior[15], M. Michalska[21], R. Moreno[27], H. Müller[3], W. Nowosielski[21], Y. Okada[3], P. Orleański[21], T.G. Phillips[20], J. Pearson[26], D. Rabois[7,8] L. Ravera[7,8], J. Rector[4], M. Rengel[9], H. Sagawa[9], W. Salomons[1], E. Sánchez-Suárez[16], R. Schieder[3], F. Schlöder[3], F. Schmülling[3], M. Soldati[15] J. Stutzki[3], B. Thomas[1] A.G.G.M. Tielens[19], C. Vastel[7,8], K. Wildeman[1], Q. Xie[4], M. Xilouris[25], C. Wafelbakker[1], N. Whyborn[18], P. Zaal[1], T. Bell[20], P. Bjerkeli[5], E. de Beck[29], T. Cavalié[9], N.R. Crockett[30], P. Hily-Blant[31], M. Kama[1,32], T. Kaminski[33], B. Leflóch[31], R. Lombaert[29], M. De Luca[27], Z. Makai[3], M. Marseille[1], Z. Nagy[1,28], S. Pacheco[31], M.H.D. van der Wiel[1,28], S. Wang[30], and U. Yıldız[19]

(Affiliations can be found after the references)

ABSTRACT

Aims. In this paper the calibration and in-orbit performance of the Heterodyne Instrument for the Far-Infrared (HIFI) is described.
Methods. The calibration of HIFI is based on a combination of ground and in-flight tests. Dedicated ground tests to determine those instrument parameters that can only be measured accurately using controlled laboratory stimuli were carried out in the instrument level test (ILT) campaign. Special in-flight tests during the commissioning phase (CoP) and performance verification (PV) allowed the determination of the remaining instrument parameters. The various instrument observing modes, as specified in astronomical observation templates (AOTs), were validated in parallel during PV by observing selected celestial sources.
Results. The initial calibration and in-orbit performance of HIFI has been established. A first estimate of the calibration budget is given. The overall in-flight instrument performance agrees with the original specification. Issues remain at only a few frequencies.

Key words. Instrumentation: spectrographs, Space vehicles: instruments, Methods: observational, Techniques: spectroscopic, Submillimeter: general

1. Introduction

The Heterodyne Instrument for the Far-Infrared (HIFI, De Graauw et al. 2010) is designed to be a very high spectral resolution receiver (R ≳ 10^6), with near-quantum limited performance for frequencies between 480 and 1910 GHz onboard the *Herschel* Space Observatory (Pilbratt et al. 2010). The high spectral resolution is mandatory for interpreting line emission as observed in a wide range of astrophysical environments with local velocity variations of only a few km s^{-1} or less. The near quantum-limited performance with an absolute calibration accuracy of 10% is needed for a detailed study of absorption lines and intercomparison of water lines in the same or different mixer bands. With the level of detail in the line profiles that HIFI provides, the physical and dynamical conditions for all gaseous material along the line-of-sight can be unraveled. The accessibility of numerous molecular lines, as well as important atomic and ionic lines, with vastly different excitation conditions allow for constraining these conditions in great detail. The wealth of molecules also allows physical conditions and evolutionary stages to be inferred by examining the chemical conditions seen with HIFI.

In this paper the calibration and in-orbit performance of the HIFI instrument are discussed and compared with the resolution, intensity, and calibration needs. A short introduction to the instrument is given in section 2 with an overview of the standard HIFI observing modes. Sections 3 and 4 describe the various parameters derived from the instrument level testing (ILT), CoP, and PV phases. Section 5 gives the overview of the HIFI observing modes and the corresponding astronomical observation template (AOT) validation. Finally in section 6, the processing tools and processing steps for HIFI data is described.

2. The HIFI instrument

The HIFI instrument is based on the heterodyne technique, where the sky signal at a frequency ν_{sky} is mixed with an ultrastable internally generated local oscillator (LO) signal at frequency ν_{LO}. These two signals are mixed in the focal plane unit (FPU) using a nonlinear mixing element. The output electrical signals contain the sum and the difference frequencies, at $\nu_{LO}+\nu_{sky}$ and at $\nu_{LO}-\nu_{sky}$. The high-frequency component is filtered away, while the difference frequency component (ν_{IF}) -

---

[⋆] Herschel is an ESA space observatory with science instruments provided by European-led Principal Investigator consortia and with important participation from NASA.

at the intermediate frequency or IF - is delivered for spectral analysis. HIFI operates as a Double SideBand (DSB) receiver, in which sky frequencies above and below the LO frequency, at $\nu_{LO}+\nu_{IF}$ and $\nu_{LO}-\nu_{IF}$, are simultaneously detected. The receiver gains for the upper and lower sidebands are not necessarily equal and thus are treated separately with their full frequency dependence. The IF signal is fed into two spectrometers: the digital autocorrelation high resolution spectrometer (HRS) and the wide band spectrometer (WBS) based on an acousto-optical spectrometer.

The frequency range of 480 GHz to almost 2 THz covered by HIFI is split into seven mixer bands, the lower frequency employing SIS (superconductor-insulator-superconductor) mixers and the two highest bands hot electron bolometer (HEB) mixers. The mixer bands are further subdivided into an upper and lower frequency subband each supplied by a different LO chain, yielding in total 14 LO subbands. Furthermore, the HIFI instrument has independent horizontal (H) and vertical (V) linear polarized signal chains to enhance scientific yield and redundancy. A more detailed description of the instrument is given in De Graauw et al. (2010).

Throughout the design and implementation phases of HIFI, high-fidelity calibration of the instrument has been one of the leading requirements. An extensive program was set to enable such high-quality calibration. The following phases can be identified as relevant for the instrument performance: 1) the subsystem tests with emphasis on characterization of the individual components and units; 2) the ILT with the emphasis on the ground characterization and calibration of the entire system with use of external stimuli; 3) the commissioning phase (CoP), an in-orbit functional check-out in which the parameters from ILT are confirmed/updated and 4) the performance verification (PV) phase in which the full scientific calibration is established. In the PV phase also the operation of the instrument in its science observing modes as laid out in the AOTs, is validated.

2.1. HIFI observing modes

The observing modes for HIFI (Table 2.1) are constructed around possible ways of taking near-real-time reference spectra. These data are required to correct for the temporal drift of the spectral response of the IF pass-band of the heterodyne spectrometer. The reference modes are a) position switch, b) dual beam switch, c) frequency switch and d) load chop. These reference modes are used by the three HIFI AOTs: 1) single point observations, 2) mapping observations, and 3) spectral scans. Since the observing efficiency is a strong function of the length of time spent to take a reference spectrum, the ratio of slewing time versus instrument stability time is an important factor in the decision process for selecting the optimal observing mode. The observation modes and AOTs are released when they are validated functionally and performance-wise. Special restrictions may apply to parts of the available frequency range. All modes, including DBS for band 5B were only released in February 2011 because of LO purity reasons (see Sect. 4.11).

2.1.1. Dual beam switch (DBS)

In this mode an internal chopper mirror within HIFI is used to move the beam to a reference OFF position on the sky. The reference OFF position is typically 3′ away from the ON-target position. Since moving the internal mirror changes the light path for the incoming waves, the possibility of residual standing waves

exists. By moving the telescope in such a way that the source appears in both (ON and OFF) chop positions, the impact of standing wave differences is expected to be eliminated. There are two chopper speeds. The faster chop is recommended for observations for low spectral resolutions where effects of instrumental drifts might be expected to distort baselines. This appears to be the case for the HEB mixer bands.

2.1.2. Position switch

In position switch reference mode the HIFI beam is pointed alternately at a target position and at a reference position with the telescope. The reference position is usually chosen to be a nearby area of the sky that is devoid of emission at the frequency being used. If emission from the reference position cannot be excluded, it must be calibrated, too. Because slewing between an ON-source and OFF-source position is time consuming, instrumental drifts are liable to reduce the overall baseline quality. Position-switch and DBS modes use equal amounts of time on the source and the reference position.

2.1.3. Frequency switch

In this mode, following an observation at a given ON frequency, the local oscillator frequency is changed by a small amount (90–300 MHz). The shift in frequency is small enough that the lines of interest remain observable at the two LO frequencies. Effectively, therefore, this makes for a very efficient mode since target emission lines are observed in both ON and OFF positions. Subtraction of the OFF spectrum from the ON means that all frequency-independent signals, including a possible continuum emission, is removed. A frequency-dependent standing wave may appear as baseline ripple after the ON - OFF subtraction. Frequency switch is not recommended in the HEB bands, owing to standing wave problems.

2.1.4. Load chop

In this scheme, an internal cold source is used as a reference. The chopping mirror alternately looks at the target on the sky and an internal source of radiation, the cold calibration load. This is particularly useful when there are no emission-free regions near the target that can be used as reference in either dual beam switch or position switch mode or where frequency switch cannot be used because of the frequency structure of the source. In frequency-switch and load-chop modes, an additional OFF position, free of emission, is highly recommended to be observed to correct for a baseline residual between the two phases.

3. Pre-flight calibration - instrument level tests

For the on-ground characterization of the entire HIFI instrument through ILT a dedicated environment was set up at SRON in Groningen. In this set-up all flight units were brought to flight-like conditions: the FPU and LOU (local oscillator unit) in dedicated cryostats and the warm units in well regulated temperature conditions. The test facility could provide dedicated test signals to the instrument by means of hot and cold shutters providing a broad band continuum signal, as well as by means of a gas cell providing spectral line inputs. The combined system was controlled by utilizing a dedicated control environment mimicking the in-flight operational environment, allowing commanding and data analysis to be done with standard observatory tools.

Table 1. AOTs for HIFI

Reference scheme	AOT/mode name		
	AOT I single point	AOT II mapping	AOT III spectral scan
1 Position switch	Mode I-1 PointPositionSwitch	Mode II-1 On-the-fly (OTF)	
2 Dual beam switch	Mode I-2 DBS and FastDBS	Mode II-2 DBS or FastDBS raster	Mode III-2 DBS or FastDBS
3 Frequency switch	Mode I-3 FSwitch	Mode II-3 OTF FSwitch	Mode III-3 FSwitch
4 Load chop	Mode I-4 Load chop	Mode II-4 OTF Load chop	Mode III-4 Load chop

All mapping modes have Nyquist or a lower sampling capability.
All dual beam switch modes have optional continuum stabilization.
All frequency switch and load chop modes have optional addition of a sky reference.

Additionally, this setup ensured that ILT data would be stored in operational databases, allowing easy access during later mission phases. Because of its close resemblance to the operational environment, the ILT setup could also be used to validate extensively all operational flight procedures, including those for the commissioning phase and routine operations as well as for the observing modes.

During the ILT, the coupling of the mixers to the hot and the cold calibration sources was measured by means of oversized, external perfect black bodies. The coupling to both hot and cold loads was found to be close or equal to unity. However, a feedback effect in the FPU via the cooled IF-amplifier box was discovered, giving excess noise up to a few percent. By covering the IF-box on the FPU with aluminum tape, the feedback effect was suppressed to less than one percent. In the laboratory all mixer beams were also accurately measured and the co-alignment was found to be within specification (see also below).

3.1. Frequency calibration

The frequency calibration measurements address both the calibration of the frequency itself (i.e. assign frequency to a given channel number of the used spectrometer) and of the frequency resolution (also called line profile). The effective instrument spectral response is the combination of several spectral element responses along the detection chain: FPU, LO, instrument controlunit (ICU) and the spectrometers (WBS and HRS).

The focal plane subsystem receives submillimeter radiation from the sky and sub-millimeter reference signals from the local oscillator. The basis for the LO signal is generated in the local oscillator source unit (LSU). A 10 MHz master oscillator (MO), designed to have frequency stability of 1 part in 10^8 over the mission lifetime, is HIFI's fundamental reference. The MO signal is distributed as a reference to the spectrometers, and is also upconverted via phase-locked synthesizers to the range 23.70 - 35.7 GHz, the first-stage frequencies for the LO covering all bands. The selected base frequency is then upconverted by a tripler to 71-106 GHz. This signal is injected in the multiplier chain of the LOU power amplifier for the active mixer band; the multiplier chains hold between two and four stages of multipliers to achieve the required radio frequency (RF)-coverage between 480 GHz and 1.9 THz. The spectral function for each band is effectively determined by the LSU upconvert oscillator used (the multiplication chain does not modify the spectral function); only bands 6 and 7 have a contribution from a secondary IF upconvert oscillator not locked to the MO, but whose contribution to frequency uncertainty is relatively unimportant. In the mixer the LO signal is combined with the sky signal, to produce the IF signal, which is passed on to the WBS and HRS. The WBS and the HRS process the signals and transmit the result to the ICU. The MO defines the frequency scale for the HRS, so the output is as correct as the MO is pure. The HRS design goal is 8 kHz accuracy, with a maximum resolution of 125 kHz (after Hanning windowing in the FFT). The spectral line response function is mainly determined by the LSU.

The WBS measures the intensity spectrum across the 4 GHz wide IF-band at 1.1 MHz resolution by combining 4 acousto-optical transducers of 1 GHz bandwidth in a single Bragg crystal. The overall spectral calibration of the AOS makes use of a measurement of an internally generated frequency "comb" of lines at known IF frequencies (between 3.9 and 8.1 GHz in steps of 100 MHz) locked to the MO. The resolution of an acousto-optical spectrometer is to a large extent determined by the properties of the acousto-optical deflector. To a lesser extent it is affected by crosstalk between the CCD elements, and by the channel spacing of the CCD elements. The channel spacing is chosen to achieve Nyquist sampling of the resolution of the spectrometer. The comb scans are repeated at intervals to mitigate frequency miscalibration related to AOS temperature drift ($\sim$ 0.1°hr^{-1} $\leftrightarrow$ $\sim$0.01 MHz hr^{-1}). This is the dominant uncertainty in frequency calibration for the WBS. The use of the combs to map CCD element to IF frequency has been found in practice to be accurate to 100 kHz or better.

Two campaigns aiming at calibrating the frequency response of HIFI were performed on the ground, first during the ILT in 2007, and second in thermal balance/thermal vacuum (TB/TV) test, in which the satellite was in the space simulator chamber at ESA-ESTEC, late 2008. In ILT, the tests were performed in lab conditions (normal air pressure, 20 °C). The frequency calibration test signal was generated using an Agilent synthesizer operating at 15-16 GHz fed into a comb generator. The comb generator produced a spectrum with a line at integer multiples of the synthesizer frequency throughout the sub-mm region up to about 1200 GHz. The output of the comb generator was used as input to the instrument via a dedicated re-imager system. To form composite (oversampled) spectra, spectra were taken with different test source frequencies: the frequency of the injected line was shifted with steps of a few kHz, resulting in an over-sampled spectrum, from which the instrument FWHM frequency resolution and frequency response function was derived. The wide band spectrometer (WBS) optics unit has been designed

Table 2. Effective LSU/HRS resolution (unapodized) as determined in ILT

Band	1a	1b	2a	2b	3a
Res. (kHz)	128	156-172	215	171	156
Band	3b	4a	4b	5a	5b
Res. (kHz)	157	216	157	156-172	156-172
Band	6a	6b	7a	7b	
Res. (kHz)	180	185	156-172	156-172	

and aligned for vacuum pressure and 10 °C, and thus the WBS-ILT results were only indicative.

The HRS spectra were also used to extract the LO line-shape by deconvolving the frequency response function. The derived LO line width was compared with that predicted from LSU characteristics as given in the end item data package (EIDP). In band 6b spectra, frequency shifts due to the free-running IF H/V local oscillator were not observed. It was concluded that the maximum effective resolution for HRS observations, including the LO-width and without apodization, ranges from 125 kHz up to 220 kHz (Table 3.1). For the WBS, an oversampled line spectrum was constructed by realigning all comb lines. It was assumed that all comb lines are the same and very narrow compared to the WBS profile and that all WBS channels have the same profile within a CCD. The comb lines from different CCDs were not mixed. From the oversampled spectrum the fluctuation bandwidth B and the resolution bandwidth D (for a definition of these quantities see Schieder & Kramer, 2001) were measured. The resulting B/D ratio varies between 1.49 and 1.54 as expected. The resolution bandwidth D varies between 1.09 and 1.11 MHz for polarization H and between 1.11 and 1.15 MHz for polarization V (hence slightly better in polarization H than in V), and in agreement with the specification ($D = 1.1$ MHz).

3.2. Sideband ratio

In an extensive measurement campaign during ILT the sideband ratio was measured as a function of frequency, employing the same technique as successfully used to calibrate the mixers of the SWAS satellite (Tolls et al. 2004). Details about the HIFI test setup and measurement concepts can be found in Teyssier et al. 2008. Figure 1 illustrates the current state of this analysis, which focused on lines of ^{12}CO, ^{13}CO, OCS, H_2O and CH_3CN (data courtesy of R. Higgins, NUIM, 2011). The normalized sideband gain ($G_{ssb} = G_{usb}/(G_{usb}+G_{lsb})$), is applicable to the calibration of lines in the Upper Sideband (USB; LSB denotes lower sideband). Most numbers indicate a sideband ratio very close to unity (i.e. G_{ssb} close to 0.5), with small local deviations, which will be fed into the HIFI calibration tree used for the HIFI pipeline processing.

Several instrumental effects led to scatter and uncertainty in the computed ratios. First of all, it was discovered at the end of the ILT campaign that the diplexers had suffered from a slight mechanical misalignment, which in practice implied an additional slope in the sideband ratio over the IF band. This misalignment was corrected in orbit but it had to be corrected for a proper retrieval of the intrinsic ratio from the gas cell data. This was taken into account for bands 3 and 4, but not bands 6 and 7 where the scatter remains. Second, several frequency ranges in HIFI had LO purity problems during the ILT. This leads to distributing the intensity of a given line over several components, and therefore to providing a larger scatter to the sideband ra-
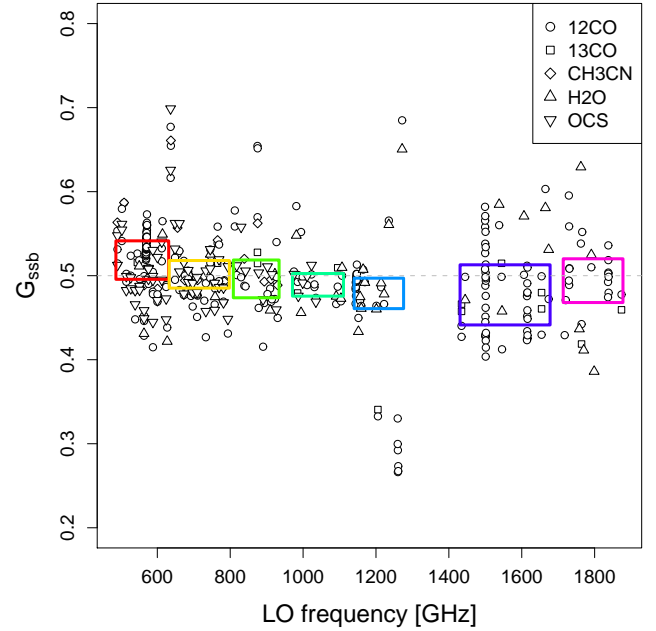

Fig. 1. Normalized sideband gain as a function of LO frequency and mixer bands (different colors)– $G_{ssb} = 0.5$ corresponds to equal gain in USB and LSB. The different gases used are indicated by the different symbols: ^{12}CO circles; ^{13}CO squares; CH_3CN diamonds; H_2O upward pointing triangles; OCS downward pointing triangles. Measurements in horizontal polarization have a black outline. The filled boxes delineate all data falling within the first and third quartiles. See text for caveats.

tio than it is in reality. This effect is particularly strong at the upper end of band 5b. Again, these imperfections have been largely solved in orbit and, sideband ratios much closer to unity have been then observed. A third source of error comes from the standing waves always present in the system. These standing waves depend both on the exact path lengths in the system (see Sec.4.12) for all bands and on the absence of an isolator in bands 6 and 7. The standing waves can influence the measurements by a few percent in the lower bands and possibly higher in the higher bands. Although errors caused in this way are generally small, the direction in which they influence the measurement cannot be determined. Finally, due to the high IF frequency (6 GHz) and IF bandwidth (4 GHz), there can be a noticeable intrinsic IF dependence of the sideband ratio in LO frequency areas where the mixer response is not flat over ranges of typically twice the IF frequency. This will be true at the edges of some of the SIS bands, and is especially observed at the lower end of band 2. In this range, additional correction factors need to be applied to the default sideband ratio to account for the intrinsic IF dependence. Appendix A describes this effect and gives some recipe to apply the additional correction. At the present time we could only confirm this theoretical effect in the first ∼ 20 GHz of the band 2, see also Higgins et al. (2010).

4. In-flight calibration - Commissioning phase

Following the launch of Herschel the performance of the satellite systems in space were checked out. Subsequently the three instruments were switched on and the instrument CoP started. For HIFI the CoP started with a functional checkout of all subsystems and characterization of basic in-flight instrument parameters. Following this the sensitivity of the system, T_{sys}, was deter-

mined. As part of the instrument characterization in this phase, a significant amount of time was spent (re-)assessing the properties of the LO system, thus determining the appropriate mixer and amplifier settings in order to get the best overall system stability.

4.1. Intensity calibration

The standard schemes for the calibration of spectroscopic measurements in radio-astronomy as described by e.g. Kutner & Ulich (1981), Downes (1988), Hiyama (1998) and Mangum (2002), mainly deal with the instability of the atmosphere, assume a narrow IF and do not consider standing waves. The ultrasensitive HIFI, with broad IF and no intervening atmosphere, has drifts and standing waves as dominant error sources. Since a full description of the HIFI intensity calibration can be found in Ossenkopf (2003, 2009), here we concentrate only on the principles of these papers and list the parameters needed for the intensity calibration.

Mounted in the cold environment of the HIFI FPU, a hot calibration source (load) is actively kept at a constant 100 K. The hot load is designed such that specular reflections are minimized, while each beam is uniformly illuminated. The cold load is a plate at the temperature of the FPU itself (12-13 K). Using these two loads for calibration is similar to the "two load chopper wheel calibration" of Hiyama (1998) and Mangum (2002). Applying such a calibration requires a number of items to be known well; 1) the zero count level of the back-ends; 2) the coupling to the calibration loads in both upper and lower sidebands η_{hot}, η_{cold} (these are not expected to differ significantly for the two sidebands); and 3) the sideband ratio, i.e. the normalized ratio of the response in the signal sideband and the combined response of the image and signal sideband (G_{ssb}). Using these numbers the Rayleigh-Jeans temperature of the loads and the measured counts in the backends, the T_{sys}, and the bandpass can be determined. When in orbit an improvement over the two-load chopper wheel calibration can be obtained by interleaving the source (ON) signal with a signal from a sky (OFF) position, which is essentially free of emission. The OFF measurement will exhibit the standing wave pattern from the round trip path between the Herschel subreflector (M2) and the HIFI mixer, modified slightly because of the different optical paths for different chopper positions. Added to these are the standing waves due to load-mixer reflections. These are again similar to the standing waves from the two-load calibration, which are absorbed in the bandpass and T_{sys}. Thus the difference of the ON and OFF spectra will effectively remove most of the optical standing waves, as long as the standing wave patterns are stable enough over the duration of the joint ON+OFF observations. In practice another measurement will be taken on a reference (REF) position, such that a double difference can be applied and all optical standing waves will be removed. In theory the REF position observing time should be comparable to the ON observing time. If the REF position does not contain any sky signal, it is possible to smooth the REF spectra such that the REF noise is reduced and only residual standing waves are retained. Depending on the different standing waves, a smoothing by a few channels up to about 20 MHz is possible. This allows for shorter integrations on the reference position.
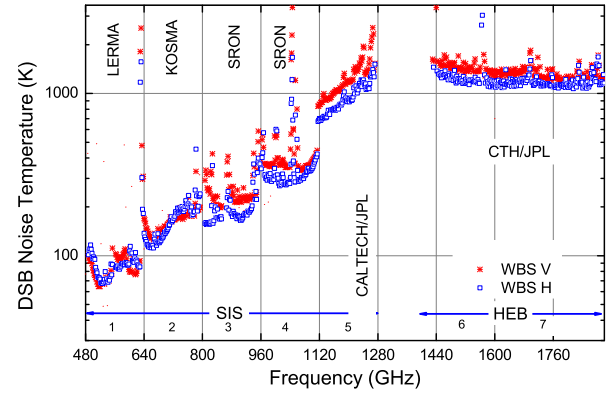

Fig. 2. System temperature of HIFI for H-polarization (blue squares) and V-polarization (red circles). The vertical bars indicate the frequency boundaries of the different mixer bands. Also indicated are the institutes responsible for the design and implementation of the different mixers.

Table 3. Allan stability times (t_A in seconds) of the HIFI instrument measured for different noise resolutions and reference bandwidths

| t_A | Continuum stability | | | Spectroscopic stability | | | | | |
| | Full backend | | | Full backend | | | 1 GHz bandwidth | | |
[s] band	native[1]	1 km/s	5 km/s	native[1]	1 km/s	5 km/s	native[1]	1 km/s	5 km/s
1a	6.5	3.5	0.8	64.0	42.0	16.0	170	120	55.0
1b	6.5	3.6	0.8	46.0	30.0	10.0	150	99	37.0
2a	14.0	8.7	2.2	71.0	48.0	16.0	300	220	93.0
2b	7.1	3.6	1.0	35.0	19.0	6.2	160	88	29.0
3a	3.4	2.1	0.7	25.0	14.0	4.8	65	40	15.0
3b	6.5	5.0	1.5	65.0	50.0	15.0	250	200	72.0
4a	1.8	1.4	0.5	9.1	7.3	2.6	120	98	38.0
4b	7.8	3.1	0.6	59.0	26.0	6.5	240	120	36.0
5a	13.0	4.4	0.9	110.0	45.0	13.0	310	160	60.0
5b	12.0	4.3	0.9	82.0	39.0	13.0	210	120	55.0
6a	1.3	0.6	0.2	11.0	4.9	1.7	32	15	5.4
6b	2.8	0.8	0.2	42.0	15.0	4.4	91	43	17.0
7a	1.5	0.4	0.1	27.0	8.9	2.5	69	25	8.1
7b	0.3	0.1	0.0	12.0	3.8	1.1	33	10	3.0

[1] the WBS native fluctuation (noise) resolution is 1.6 MHz

4.2. Sensitivity

The most important parameter determining the sensitivity of HIFI is the overall noise level of the receiver system characterized by the system temperature T_{sys}. Scans of the hot and cold loads were taken over the entire HIFI range retuning the LO with steps of about 4 GHz. From these scans the median value of T_{sys} over the full IF bandwidth was determined by applying the standard radiometric analysis (Fig. 2). Overall, the system was found to be as sensitive as or even slightly better than what was measured during the ILT campaign on ground, and thus compliant with the original instrument requirements. No evidence has been found of a direct detection effect in the HEB bands 6 and 7.

4.3. Stability times

HIFI, like all heterodyne receivers, exhibits instrumental drifts in each of its 14 mixer band IF output channels. To suppress these drifts, reference spectra that can be subtracted from the science measurements need to be obtained either by looking off source, at one of the stable loads, or by switching to a nearby frequency

at suitable time intervals. The susceptibility of the instrument to drifts can be described by the stability time derived from the Allan variance spectrum (Allan 1966). Stability over the resolution bandwidth (the spectroscopic stability time), the complete WBS 1GHz subbands, or over the complete IF (total power stability time) can be measured. The Allan stability measurement compares the instrumental drift with the radiometric noise; after one Allan time, radiometric noise and drift noise contribute equally to the uncertainty of the data. An optimum measurement cycle should last about 1/3 of the Allan time (see Ossenkopf 2008 for details).

Table 3 lists some relevant stability times for the HIFI bands, obtained by analyzing the cold blackbody signal. The Allan stability time decreases with radiometric noise as the target spectral resolution bandwidth is increased. The stability numbers at the native resolution and when binning only a few channels are quite reliable and reproducible. When aiming at larger goal resolution bandwidths, the actual instrument behavior becomes more uncertain. Observations aiming at large binning widths are always in danger of being affected by individual thermal drift events. Due to the statistical nature of the description used in the Herschel observation planning tool HSPOT, the predictions are close to the actually measured values when integrating for a long enough time, i.e. for at least an hour, but for short observations large deviations from the predicted uncertainty are possible. Those uncertainties express themselves as baseline distortions that can be reduced by some baseline smoothing algorithm for narrow enough lines.

4.4. Beam calibration

The Herschel telescope is described in Pilbratt et al. (2010). Although the largest in space, the telescope (or antenna, in radio terms) poses a physical limit on the detail that can be seen on the sky. The obtained intensity distribution is the sky brightness folded with the antenna pattern. The hot-cold calibration provides an intensity (temperature) scale. To obtain antenna-independent sky-brightness temperatures, knowledge about the antenna pattern and the involved efficiencies is required. A full model of the telescope system could be used, but for the HIFI calibration we rely on knowledge of celestial sources, in particular Mars. With dedicated observations of well known sources antenna parameters, such as half-power beam width, the beam profile and telescope efficiencies can be determined. The results on beamwidth, edge taper, aperture efficiency, and beam efficieny listed below are derived on the assumption of Gaussian beams without accounting for the central obscuration and assuming source sizes close to the size of the beam. Part of the energy received by the Herschel-HIFI combination comes from outside the main lobe of the point spread function. Therefore to measure the full beam profile, one of the brightest objects available to Herschel, the planet Mars, was observed. The characterization of the Herschel telescope point spread function (PSF) by PACS (Pilbratt et al. 2010, and Poglitsch et al. 2010) gives confidence that the Herschel optical system performance is close to the design specifications.

4.5. Chopper calibration

The focal plane chopper (FPC), a rotatable mirror that can change the orientation of the telescope beam on the sky, makes it possible to chop between an ON- and OFF- source sky position within 40 ms. The FPC is also used to allow the HIFI detectors

Table 4. HIFI theoretical beam-size and co-alignment of the HIFI H and V mixers

Band	ν GHz	λ mm	FWHM $''$	Δ(H-V) [†] Y $''$	Z $''$	Coupling loss %
1	480	0.625	44.2	−6.2	+2.2	1.5
2	640	0.469	33.2	-4.4	-1.3	1.3
3	800	0.375	26.5	-5.2	-3.5	3.8
4	960	0.312	22.1	-1.2	-3.3	1.7
5	1120	0.268	18.9	0.0	+2.8	1.5
6	1410	0.213	15.0	+0.7	+0.3	0.2
7	1910	0.157	11.1	0.0	-1.0	0.6

[†] Y and Z are spacecraft coordinates.

to observe the hot and cold calibration loads inside the FPU. The mechanism accuracy of the FPC, hence its mirror during observations, is better than $3''$, which translates into a position accuracy of approximately $0.03''$ on the sky. A $4.9°$ rotation of the FPC mirror provides a $3'$ rotation of the telescope beam on the sky. In practice there are very small differences in the alignment of the optics of the seven frequency bands, for which the chop angles have been corrected.

4.6. Mixer co-alignment

Each HIFI mixer band consists of H and V polarized mixers mounted in separate subassemblies. Great care has been taken in aligning the H and V polarization beams, thus allowing the two beams to be averaged to improve the overall signal-to-noise ratio. In Table 4 the distance between the two mixers for each band in angle on the sky in the Y and Z spacecraft-coordinates is given. The coupling losses compared to perfect co-alignment are also indicated.

4.7. Aperture and beam efficiency

To characterize the HIFI beam and aperture efficiency at different frequencies, 7×7 raster observations of the planet Mars were carried out. The frequencies were chosen such that the beam could be characterized well for all LO sub-bands. After standard pipeline processing two-dimensional Gaussian profiles were fit to the Mars images to determine beamwidths. The beamwidth was found to be in excellent agreement with the values predicted based on the Herschel telescope parameters; the HIFI beam varies between $45''$ at 490 GHz and $11''$ at 1.9 THz following a linear frequency dependence, with the exception of Band 5, where a larger beam is found, possibly because of the extra optical element, "monocle", added to fix polarization issues of the sapphire substrate/silicon lens combination. With the HIFI intensity calibration and model fluxes for Mars[1], the data also allowed determination of the aperture efficiency. The numbers found from the Mars measurements do agree very well with the numbers derived from the ILT beam measurements (propagated to the sky by a telescope model) given in Jellema et al. (2011), which give $\eta_A = 0.66 \pm 0.03$ for band 1H.

Main beam efficiency and aperture efficiency follow a wavelength dependence given by a Ruze formula:

$$\eta_{mb} = \eta_{mb,0} \cdot \exp\left[-(4\pi\sigma/\lambda)^2\right] \tag{1}$$

$$\eta_A = \eta_{A,0} \cdot \exp\left[-(4\pi\sigma/\lambda)^2\right]. \tag{2}$$

---

[1] http://www.lesia.obspm.fr/perso/emmanuel-lellouch/mars/

Table 5. Recommended values for beam efficiency, aperture efficiency, half power beam width (HPBW), and point source sensitivity (S/T_A^*).

Band	ν	$\eta_{mb,\nu}$	$\eta_{A,\nu}$	HPBW	point source sensitivity
	GHz			″	Jy/K
1	480	0.76	0.68	44.2	464
2	640	0.75	0.67	33.2	466
3	800	0.75	0.67	26.5	469
4	960	0.74	0.66	22.1	472
5	1120	0.64	0.56	18.9	558
6	1410	0.72	0.65	15.0	485
7	1910	0.69	0.62	11.1	506
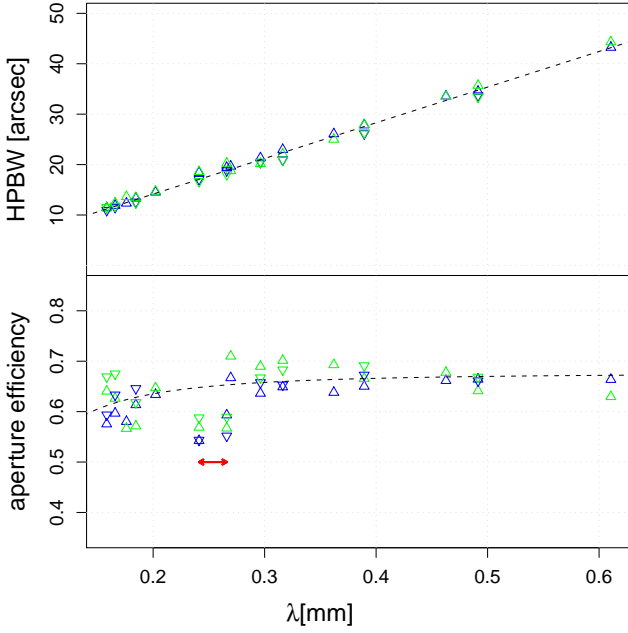
Fig. 3. HPBW and aperture efficiencies observed as a function of wavelength towards the planet Mars. Blue and green symbols represent observed values for horizontal and vertical polarization, respectively, whereas up and down pointing triangles distinguish two different observing runs. The black dashed lines represent fits to the relations described by Eqs. 3 and 1, resp. Observations in band 5 (marked with the red arrow) were excluded from the fit to the aperture efficiencies.

For bands 1–4, 6 and 7 we find $\eta_{mb,0} = 0.76 \pm 0.02, \eta_{A,0} = 0.68 \pm 0.02$ with $\sigma = 3.8 \pm 0.9\,\mu$m; for band 5 these numbers are $0.66 \pm 0.02, 0.58 \pm 0.02$ and $3.8 \pm 0.9\,\mu$m with λ in μm. The relation between aperture and main beam efficiency is given by: $\frac{\eta_{mb}}{\eta_A} = \frac{A_{\text{geom}}\Omega_{mb}}{\lambda^2} \approx \frac{\pi D^2}{4}\frac{\pi}{4\ln 2}\frac{\theta_b^2}{\lambda^2}$, with A_{geom} the effective surface of M1, with $D = 3.28$ m; Ω_{mb} the beam solid angle and θ_b the HPBW.

The measured beamwidths for HIFI are given by

$$\theta_B(\text{rad}) = \frac{2}{\pi}(1.6 + 0.021 \cdot T_e(\text{dB})) \cdot \frac{\lambda}{D} \qquad (3)$$

with $T_e = 7.94 \pm 0.82$ dB as the measured edge taper, and λ the wavelength in m. For Herschel D=3.28 m. The forward efficiency is 0.96.

4.8. Focal plane geometry and pointing

During PV, two focal plane geometry tests were done in which point sources were mapped, leading to changes in the spacecraft instrument alignment matrix (SIAM), such that sources always appear within the pointing accuracy. See Pilbratt et al. (2010) for Herschel results based on PACS observations. Routine pointing checks during the first 1.5 years show no deviations.

4.9. Frequency and velocity calibration

After launch, the detailed spectral response of a spectrometer channel cannot be measured in orbit owing to the lack of sweepable, narrow band signals. Spectral lines from suitably well-characterized sources were used to confirm the frequency calibration. Sources observed at multiple epochs serve as 'internal' calibrators, confirming HIFI self-consistency. Emission lines from circumstellar envelopes observed with the APEX telescope (Atacama Pathfinder EXperiment) were used as external calibrators (Risacher & van der Tak 2009) and twenty AGB stars were observed in the CO $J = 6$–5 line, which is visible in HIFI band 2. The frequencies are consistent within the uncertainty provided by the signal-to-noise of the line detections .

Additionally, a large number of lines observed by HIFI during PV have been checked in terms of frequency/source velocity consistency, repeating some observations several times and performing those with different observing modes. In all cases, the frequency was as expected, and the observed line profiles were consistent with those observed with APEX or found in the literature.

In orbit, the functional check of the WBS confirmed the performance parameters measured in the on-ground ILT: resolution D <1.1 MHz, noise fluctuation bandwidth B ≤1.65 MHz, and stability time scale (Allan variance minimum time) t_A > 200 s. The trend toward a slowly decreasing intensity of the frequency comb in the V-polarization, which was already observed on ground during the ILT, continues at the expected rate. This decrease is due to a gradual loss in gain of the comb, but is not expected to become critical during the lifetime of the mission, especially since an operational procedure exists that couples the HRS calibration to the WBS. It was also confirmed in orbit that, with the automatic leveling of the IF power, the WBS can cope well with the wide dynamic range of > 30 dB necessary for the various observing conditions.

The thermal conditions are critical for the stability of the spectrometer, hence for the overall science performance of the instrument. It was found that the thermal environment in the service module in orbit was not within specifications. Significant thermal drifts are introduced by the switching of other Herschel components and, in particular, of an electronics unit from the SPIRE instrument. Operational procedures have been redefined to adapt to this situation such that the stability requirements for the WBS are met in the periods when HIFI is used for routine operations.

A final source of uncertainty that has to be taken into account in the frequency assignment for both spectrometers is the velocity determination of the spacecraft. This requires good knowledge of the spacecraft orbit and the orientation of the orbit with respect to the line of sight towards observed sources. The spacecraft velocity is reconstructed with an accuracy better than $1\,\text{m s}^{-1}$, and the intended pointing accuracy is 2 arcseconds. These small velocity line-of-sight uncertainties contribute less than 10 kHz of error at HIFI's highest observing frequency.

Determining HIFI's frequency calibration consistency over time is the subject of monitoring observations. The tests so far indicate that the accuracy of the derived inertial frequencies is 100 kHz or better (WBS; ~50 kHz or better for the HRS), and there is no evidence of any systematic difference with respect to ground observations (*ie* APEX).

4.10. Diplexer calibration

For four of the mixer bands, diplexers in the FPU provide LO and signal coupling. These diplexers are unbalanced, hence need re-adjustment once in zero gravity (in flight). The diplexer calibration starts with a coarse tuning to optimize the LO-mixer coupling. Neither the optimum LO power nor the optimum diplexer setting is known a priori, so the diplexer scan is executed for 7 LO power settings to find at least one proper setting. The LO output power is controlled by the drain voltage setting of the second stage power amplifier in the chain, before the multipliers. This drain voltage-mixer current relation is needed for the diplexer fine calibration, in which the diplexer setting for the signal path is optimized. The reason for including this test is that cross-polarization effects at the beamsplitter and diplexer grids mean that the diplexer tuning for a particular LO subband is different than for the sky path. However, since the two LO subbands operate at ±45° relative to the mixer polarization, this effect can be calibrated out, and the diplexer tuning for unpolarized signal from the sky directly results from the LO port diplexer calibration. The signal path coupling is finally confirmed by a hot-cold calibration procedure, as well as by inspection of the noise-temperature distribution across the IF-band. Generally, the fine-tuning confirms the coarse calibration results. The final accuracy is better than 2% of a wavelength, so the signal coupling losses are negligible. Besides the optimal diplexer setting, an optimal LO power also exists. In HIFI we have chosen to optimize for the H-mixer.

4.11. Purity of the LO signal

Laboratory testing of HIFI revealed a number of local oscillator settings where the receiver showed response at undesired frequencies. The origin of these deviations was traced to parametric oscillations in the first or second stage doublers in various multipliers. The laboratory testing results and in-flight characterization and optimization has identified and in most cases eliminated the oscillations. The program to eliminate the parametric oscillation was carried out in bands 1b, 3b, 5a, 5b, 7a, and 7b. At the time of the last update (May 2011), only those regions with LO frequencies above 714 GHz (band 2a); around (±1 GHz) 941 and 952 GHz (band 3b); above 1114 GHz (band 4b); around (±2 GHz) 1135 GHz; below 1236 GHz and around (±1 GHz) 1255 GHz (band5b); and between 1755-1759 GHz (band 7a) were still affected. Occasionally data taken at LO frequencies close to the spurious frequencies are seen to have excess noise. Deviating SBRs are also possible.

4.12. Standing waves

Standing waves are common in sub-mm instruments because the wavelength of the radiation is comparable to the telescope optics dimensions. A standing wave occurs when a fraction of the incoming signal is reflected back along the optical path and then reflected again back along the signal path towards the detector. The round trip distance between the two reflecting surfaces de-

Table 6. Optical standing waves in HIFI and their approximate relative error contributions.

Period (MHz) Source Band	92 & 98 CBB& HBB (%)	100 LO (%)	620 DRTM (%)	Overall impact (%)
Band 1	3-4	<1	-	4
Band 2	3-4	<1	-	4
Band 3	1-2	2-4	1-2	4
Band 4	1-2	2-4	1-2	4
Band 5	1	3	-	3
Band 6	<1	3	-	3
Band 7	<1	3	-	3

The errors caused by the standing waves are derived from continuum observations of Saturn. Careful inspection of the standing waves over the whole IF allows for classifying them and assessing the individual impacts. The overall impact column gives the impact as assessed over the whole IF rather than an RMS (root mean square) of the individual errors. In bands 6 and 7 excursions attributable to the LO-mixer standing wave have been seen up to 25%. All values given here are peak-peak values divided by 2.

termines the phase delay between the incoming and reflected signals. These two signals interfere and modulate the intensity detected at that sky frequency.

In HIFI, standing waves are seen in a number of ways. The "classic" standing waves are those seen in the sky signal path, and they appear as a modulation of the spectrometer baseline. The most common source of standing waves is the cavity between the detector (mixer) focus and the secondary mirror. This effect was considered in the design of the Herschel secondary mirror. A scatter cone was incorporated into the secondary mirror that almost completely removes this potential standing wave source. Unfortunately HIFI still has a number of standing waves in the internal optics. These standing waves, especially visible when no reference position is used in the observation, occur between the mixer focus and the cold black body (CBB), the mixer focus and the hot black body (HBB), the mixer focus and the diplexer roof top mirror (DRTM), the LO and the mixer, and within the IF chain. Approximate errors caused by the optical standing waves are given in Table 6 .

The cavity length can be determined by measuring the period of the standing wave. By comparing this length with the instrument optics dimensions, one can determine the source of reflection. The cavity length d is determined from the relation, $d = c/(2P)$, where P is the standing wave period in MHz and c is the speed of light. A dedicated series of tests were executed to characterize the various standing waves present. Table 6 gives a summary of the optical standing waves occurring in HIFI.

The 320 MHz standing wave seen in bands 6 & 7 is different from the other standing waves listed in Table 6. This standing wave period has no corresponding cavity in the HIFI optics. Further investigation shows that this standing wave period corresponds to the coaxial cable length between the mixer and the first low-noise amplifier. Unlike bands 1 through 5, bands 6 and 7 have no electrical isolator between the first amplifier and the mixer and therefore are more susceptible to IF power reflections due to the impedance mismatch between the mixer and amplifier. The real and imaginary reflection and transmission properties for the mixer and amplifier vary significantly across the IF band width resulting in a complex standing wave profile. This profile is difficult to fit with a sinusoid, so more sophisticated
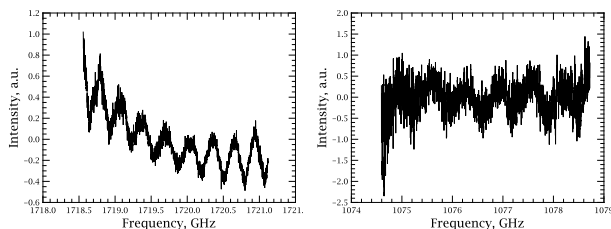
Fig. 4. Examples of the 320 MHz standing wave seen in the HEB IF chain(left panel) and the 680 MHz standing wave due to reflection between the mixer focus and the diplexer rooftop mirror (right panel)
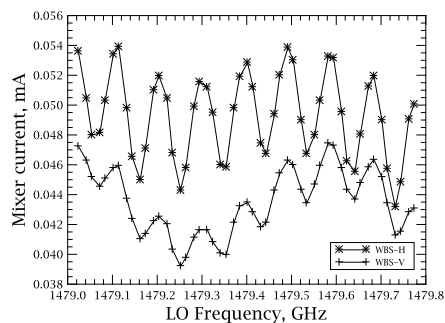

Fig. 5. Plot of the mixer currents for both H and V mixers. For this test the LO power is kept constant and the LO frequency is changed. In this plot two standing waves are apparent; a 92 MHz modulation corresponding to a distance between the LO source unit and the mixer focus and a 680 MHz period standing wave corresponding to a reflection between the diplexer rooftop mirror and the mixer focus.

approaches have to be implemented. This topic is discussed in detail in Higgins et al. (2009). An example of the HEB band baseline distortion is shown in Fig. 4 to the left. An example of an optical standing wave due to diplexer roof top mirror reflection is shown in Fig. 4 to the right.

The baseline modulation shown in Fig. 4 is an example of the obvious effect of standing waves on the final data quality. A second, more subtle type of standing wave occurs in the LO signal path. Standing waves in the LO signal path modulate the LO power pumping the mixer and cause a modulation of the mixer sensitivity. These effects can be detrimental to frequency switch observations where, depending on the frequency throw, there can be a significant power difference between ON and OFF positions, resulting in a poor pass-band subtraction. Figure 5 shows an example of the modulation on the mixer pumping level when the LO power is fixed and the LO frequency is changed. The effect of LO path standing waves on a heterodyne system is discussed in detail in Siebertz et al. (2007).

4.13. Calibration error budget

The HIFI calibration closely follows Ossenkopf (2003). From the equations in this paper formal errors can be derived for the parameters involved (sideband ratio, hot and cold load coupling, hot and cold load temperature) with their respective weighting. Also of influence are knowledge of the planetary model, the aperture or beam efficiency, the pointing of the Herschel satellite, and finally the impact of the standing waves. In Table 7 an overview is presented of these uncertainties.

Following Ossenkopf (2003) the errors can be combined into an overall error by assuming all errors are independent. However, such an error would be a gross overestimate since

Table 7. Relative (percentual) calibration error budget for the HIFI Instrument.

| Error source | HIFI mixer band | | | |
	1 & 2	3 & 4	5	6 & 7
Sideband ratio	3-4	4-6	4	5-8
Hot load coupling[1]	<1	<1	<2	<3
Cold load coupling[1]	<1	<1	<2	<3
Hot load temp.	<1	<1	<1	<1
Cold load temp.	<1	<1	<1	<1
Planetary model	<5	<5	<5	<5
Beam efficiency	<5	<5	<10	<5
Pointing[2]	<1	<3	<4	<8
Opt. standing waves	4	4	3	3

[1] The coupling error in bands 6 & 7 is likely an overestimate and may include standing wave effects.
[2] This relative intensity error is given for an Absolute Pointing Error (APE) of 2″ for a single point observation of a point source.

all HIFI measurements, from ILT-data on the load couplings to routine calibrations of Mars, have standing-wave contributions. Also small mixer current variations and small alignment errors can lead to extra deviations. Therefore it is better to assess the consistency of measurements over several epochs between February 2010 and May 2011. This has not been done in a systematic fashion, but spot checks show lines in HIFI to be equal to within 10%.

4.14. Single event upsets

HIFI has three areas where it is susceptible to single event upsets (SEUs), commonly believed to be caused by high-energy cosmic rays. Twice per year a bit-flip is observed in the memory areas of the ICU, which may lead to an autonomous stop in observations if HIFI is observing. Switching off and on of the power lines to the ICU and subsequent reloading of the OnBoard SoftWare (OBSW) re-enables the functioning of the ICU.

SEUs in the memory banks of the LCU microprocessor are much more frequent, approximately once per 13 days. After the OD81 anomaly (Jellema et al. 2010), extra care was given to handling SEUs in this microprocessor. The memory of the microprocessor is divided into three areas: safe, table, and critical, all monitored by separate checksums. SEUs in the safe area do no harm and are removed by uploading a new image of the memory. SEUs in the table area can affect the safety limits of the operation of a pair of LO Chains. However, implemented hardware limits protect the chains and will prevent damage. Every pair (H and V) of LO chains takes approximately 1/7 of the table area. If an SEU occurs, the operating band is generally not affected. If it is, HIFI stops operations until a new memory image is uploaded during radio contact and some science time is lost. If an SEU occurs in the critical area, the LCU has to be switched off and on in the daily radio-contact period. Science time is usually lost, since the LCU will be in an unknown state and may or may not keep communicating with the ICU.

The last area of possible susceptibility is the Bragg cell of the WBS. Occassionally, showers of electrons have been detected in HIFI spectra. No permanent damage has been noted from these events.

9

5. Validation of the HIFI astronomical observing templates

An extensive program of observing mode and AOT validation was executed. All AOTs were exercised on different types of sources and at different frequencies to explore the full parameter space of instrument settings available to the astronomers. In total over 100 observations were carried out, many of galactic line-rich sources, but also of solar system objects and external galaxies. All individual observations were analyzed for noise properties, standing wave signatures, line strengths as compared to model predictions, etc. Data reproducibility was also verified by repeating some observations and by cross comparing observations of the same source using different modes. By careful planning and an aggressive program for analysis and interpretation of the initial AOT data the Instrument Control Center could, already 2.5 months after HIFI was switched on in January 2010, declare the DBS mode validated for science operations. Soon thereafter the frequency switch, load chop, and mapping modes were released for science operations as well. Some operational caveats do remain, summarized in this paper and in notes available at the Herschel Science Center website[2]. Furthermore, care has to be taken at a number of frequencies where spurious LO signals are present. The affected frequencies are well documented, and the user is warned by the observation planning tool if an observation is likely to be affected. Since the band 6 and 7 HEB mixers show low stability times, fast referencing should always be used in these bands. Slow referencing will lead to data that cannot be properly calibrated. Similarly the stability of these bands is such that frequency switching is found not to be effective, also leading to data that cannot be properly calibrated.

5.1. HIFI astronomical observing templates (AOT)

5.1.1. Point source AOT

This AOT is designed for pointed observations and in certain cases to make very small maps. It can utilize all four observing modes as described above.

5.1.2. Mapping AOT: on-the-fly (OTF) and raster mapping

On-the-fly mapping is probably the most efficient means of collecting data to map emission over a large region of sky. Data are taken continuously while the telescope is scanned back and forth across the target with data readouts taking place at a scanning distance similar to the beam size at the frequency of observation. A single emission-free point reference position measurement is used as an OFF measurement. Frequency switching is also available for OTF mapping. In raster mapping, DBS observations are carried out at successive map positions on a regular grid.

5.1.3. Spectral scans AOT

This AOT is designed for making spectral scans for a part or the whole of a frequency band. Typically these are made at LO frequencies that are approximately 1 GHz apart. For each observing frequency setting, DBS or frequency switch measurements can be made, resulting in fully calibrated dual sideband spectra at each of the LO settings. The creation of a single sideband spectrum is achieved afterwards by a deconvolution routine during data processing (Comito & Schilke 2002).

---

[2] http://herschel.esac.esa.int/

6. HIFI data analysis

To allow scientific interpretation of HIFI observations, the raw HIFI telemetry needs to be converted to fully calibrated spectra. Much of this can be done using the standard HIFI pipeline processing software as distributed with the Herschel interactive processing environment (HIPE, Ott 2010). HIPE also provides tools to assist with further analysis and interpretation of HIFI observations, e.g., through line fitting and identification functions.

6.1. The HIFI pipeline

The HIFI pipeline consists of four stages of processing leading to four HIFI data levels. The processing steps are designed to associate satellite information with HIFI telemetry, to frequency-calibrate the raw spectra arising from the two spectrometers, and to apply the reference spectra to the data as dictated by the observing mode (see Sect 2.1). The processing is summarized here. A more detailed description of the pipeline processing steps is given in the documentation delivered with the HIPE software.

6.1.1. Level 0 processing

The first processing stage, the level 0 pipeline, converts the raw telemetry from HIFI into the appropriate format for further processing. In this stage checks are also performed to verify that the mixers were properly pumped during the observation, that the LO was within appropriate limits, and that all the dataset is complete and consistent. Additionally, the satellite pointing information is interpolated to the individual telemetry read outs, and further satellite information associated with the observation is collected and attached (e.g., uplink information or out-of-limits information). The resulting level 0 pipeline product contains all the information necessary for later reprocessing. This pipeline stage is identical for WBS or HRS spectrometers and independent of observing mode.

6.1.2. Level 0.5 processing

In the second stage, the level 0.5 pipeline, spectrometer specific calibrations are applied and the spectrometer specific signatures which are present at level 0 are removed. For WBS data this process entails the following steps; 1) normalize the integration times, 2) check for saturation, 3) subtract the dark values, 4) apply the CCD non-linearity correction, 5) apply an interpolated zero correction, 6) derive the frequency scale from the comb spectra, 7) correct the intensity scale for the applied attenuator settings, 8) split the spectra into subbands and 9) check the cold calibration spectra for spurs and flag potentially affected channels. HRS data are first split into HRS subbands and subsequently processed using the following steps: 1) calculate the offset and power of the analog input signal, 2) normalize the correlation functions, 3) correct for the quantization distortion, 4) correct the gain for nonlinearity, 5) apply a Hanning windowing when requested, 6) symmetrize the correlation functions, 7) apply a Fourier transform to the correlation functions in order to convert to HRS power spectra, 8) Hanning-smooth the spectra, 9) calculate the frequency scale, 10) correct the spectra for IF nonlinearity, and 11) cut the edges of the HRS spectra according to the bandpass of the filters.

6.1.3. Level 1 processing

The data sets for both spectrometers need further processing to level 1 products. The exact processing depends on the observing mode. First another sanity check is again performed on the data structure, and the following steps are subsequently applied: 1) analysis of the LO groups for either frequency switch observations or drifts in frequency scale, 2) analysis of the observation pattern found in the data to verify that they match the AOT, 3) calculation of the bandpass and system temperature, 4) subtraction of the reference (clearly this step is dependent on the observing mode used), 5) computation and subtraction of a baseline from the OFF positions if applicable, 6) intensity calibration based on internal loads, and 7) velocity correction to the frequency scale from the spacecraft reference frame to the LSR reference frame.

The design of the HIFI pipeline is such that all "hands off and blind" processing is done in the steps leading up to this level 1 data product. There should be little need to alter the steps currently applied. However, experience has shown that additional spur finding and removal as well as a dedicated standing wave removal step, may be needed to further improve the data quality.

6.1.4. Level 2 processing

The level 2 pipeline is comprised of those steps that depend on observing mode (single-point integration, mapping, or spectral survey, see Sect.5.1). For example, if the observation mode is a "Point" mode, all the level 1 spectra will be averaged to form the level 2 data product, and a level 2 data cube will be generated for the mapping modes. Since these steps are done in a hands-off automated pipeline, it is important to inspect the level 1 products to determine if the level 2 process was appropriate. The level 2 product best serves as a quick look at the observation and can provide some clues into which issues (for example standing waves) might be present in the data that require more careful processing.

Currently the level 2 pipeline performs the following steps: 1) removal of unnecessary information from the data products, 2) application of the forward efficiencies and sideband gain coefficients, 3) generation of separate upper and lower sideband spectra, 4) resampling to a linear frequency grid, and 5) creation of data cubes (for each subband and sideband) for mapping modes or average spectra for pointing modes. It should be noted that the ordering and parameters for the steps in the level 2 pipeline are constantly being refined.

6.2. Further analysis

Spectral surveys can be processed through the double sideband deconvolution algorithm to produce a single sideband spectrum covering the entire frequency range of the observation. The HIFI experts at the instrument control center (ICC) are investigating the performance of the deconvolution step, and as yet it is not part of the automatic level 2 pipeline. Additional steps include unfolding frequency-switched data, stitching subbands, finding and removing spurs, identifying and removing standing waves, fitting various types of line profiles and automatically identifying line species. Most of these operations are available in the HIPE system and some may well become part of the standard pipeline process.

7. Conclusions

The initial in-flight characterization and calibration of the HIFI instrument has been completed. The instrument is found to perform according to its specifications in terms of sensitivity, spectral line profile properties, and stability, as well is in its modes of operation for scientific observations. As a result HIFI shows very good reproducibility, leading to the conclusion that the baseline requirement on calibration is achieved for most frequencies. The formal goal calibration error of 3% is likely not to be reached with Herschel-HIFI. To achieve this, new heterodyne missions would profit from off-axis telescope design, single sideband mixers or sideband separating mixers, beamsplitters rather than diplexers with rooftop mirrors, and calibration loads for which the reflection coefficients are accurately measured.

Appendix A: Intrinsic sideband ratio IF dependence

When the gain response of a DSB heterodyne mixer is not equal in its respective upper and lower side bands, the so-called sideband ratio (SBR = G_{usb}/G_{lsb}) deviates from unity. Since gain responses are usually smooth functions of the LO frequency, one can assume to first order that this gain function is approximated to a nearly constant slope over a frequency range extending typically from $\nu_{LO} - \nu_{IF}$ to $\nu_{LO} + \nu_{IF}$, where ν_{LO} and ν_{IF} are the LO and IF frequencies, respectively. In this assumption, one can demonstrate that IF frequency points farther away from the LO frequency will have a more unbalanced sideband gain than those closer to the LO frequency. This is illustrated in Fig. A.1. In this model, an SBR of e.g. 1.16 is assumed at $\nu_{LO} = 570$ GHz and $\nu_{IF} = 6$ GHz. One can see that the SBR would vary between 1.1 and 1.22 from one end of the IF to the other.

In this formalism, one can demonstrate that the IF variation of the SBR can be described as

$$\text{SBR}(\nu) = (\text{SBR}_{IF})^{\nu/\nu_{IF}} \qquad (A.1)$$

where SBR_{IF} is the SBR at ν_{IF} (i.e. in the middle of the IF band). Figure A.2 shows the typical error that would affect SBR over the IF band if one assumed that the SBR value at the IF center applies over the whole IF bandwidth.
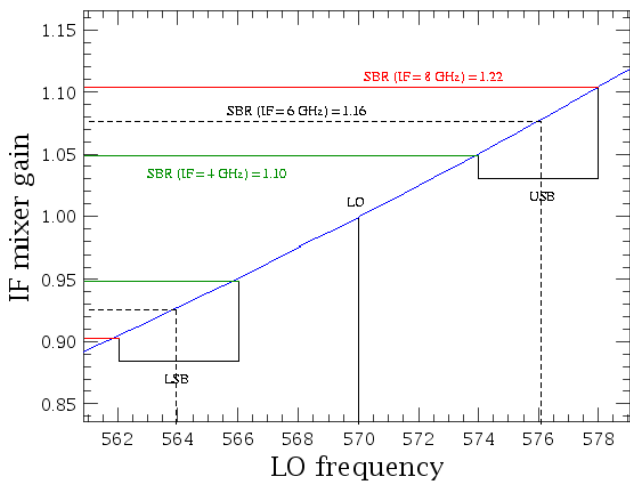
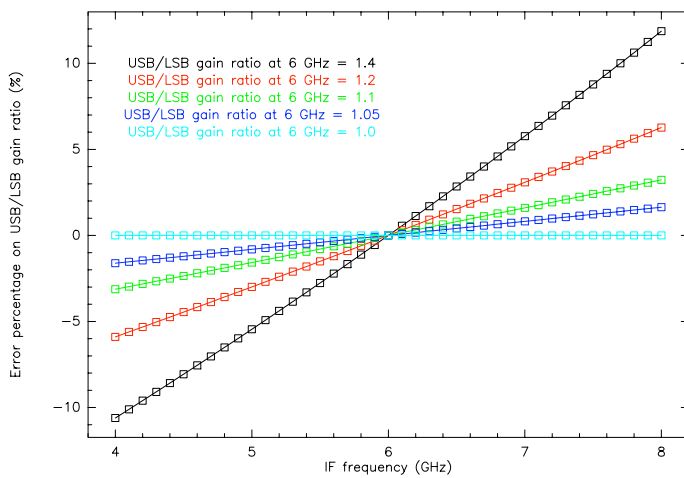**Fig. A.1.** Deviations in sideband ratio with large sideband separation

Fig. A.2. Errors resulting from deviations in sideband ratio with large sideband separation

Of course, such intrinsic correction should be applied with extreme care, since the assumption of a smooth and constant slope response over a large section of the mixer frequency range is not always guaranteed despite evidence of large SBR deviations at spot frequencies. For instance, inflexion points in the gain function can lead to a similar situation with a mixer response that is far from a straight line over, e.g., twice the IF. For the case of HIFI, we have observed that this formalism was accurate at least in the lower end of band 2a (see section 4.2). This effect should at least be kept in mind, in particular when analyzing features in spectral scans where the lines are measured at several, often extreme, positions in the IF.

References

Allan D.W. 1966, Proc. IEEE 54, no. 2, 221
Comito, C., & Schilke, P. 2002, A&A, 395, 357
de Graauw, T., Helmich, F.P., Phillips, T.G. et al. 2010, A&A, 518, L4
Downes, D., 1988, in: Appenzeller, I., Habing, H.J., Lena, P., Evolution of galaxies - Astronomical Observations, Lecture Notes in Physics 333, p. 351
Higgins, R.D., Kooij, J.W., 2009, Society of Photo-Optical Instrumentation Engineers (SPIE) Conference Series 7215, 15
Higgins, R.D., Teyssier, D., Pearson, J.C., Risacher, C., Trappe, N.A., 2010 in: 21st International Symposium of Space Terahertz Technology, University of Oxford and STFC Rutherford Appleton Laboratory, 390
Higgins, R.D., 2011, "Advanced optical calibration of the Herschel HIFI heterodyne spectrometer", PhD thesis
Hiyama, S., 1998, Diploma thesis, Universität zu Köln
Jellema, W.J., Jacobs, H., Van Leeuwen, B.-J., et al. 2010 in: The 21st International Symposium on Space TeraHertz Technology, held March 23-25, 2010 at Oxford University's Said Business Center and the STFC Rutherford Appleton Laboratory, Oxford, UK. National Radio Astronomy Observatory (NRAO), p.33-39
Jellema, W.J., 2011, Appl. Optics, in preparation
Kutner, M.L., Ulich, B.L., 1981, ApJ 250, 341
Mangum, J., 2002, Load Calibration at Millimeter and Submillimeter Wavelengths, ALMA Memo Series 434
Ossenkopf, V., 2003, The HIFI intensity calibration framework, ALMA Memo Series 442
Ossenkopf, V., 2008, A&A 479, 915
Ossenkopf, V., 2009, A&A 495, 667
Ott, S. 2010, ASP Conference Series, 434, 139
Pilbratt, G.L., Riedinger, J.R., Passvogel, T. et al. 2010 A&A, 518, L1
Poglitsch, A., Waelkens, C., Geis, N. et al. 2010, A&A, 518, L2
Risacher, C., Van der Tak, F., 2009, ALMA-ALLEGRO memo 2, http://www.alma-allegro.nl/images/memo2.pdf
Schieder, R., Kramer, C., 2001, A&A 373, 746
Siebertz, O., Honingh, C., Tils, T., Gal, C., Olbrich, M., Bieber, R., Schmuelling, F., Schieder, R., 2007, 18th International Symposium of Space Terahertz Technology, California Institute of Technology, Pasadena, California, 117
Teyssier, D., Whyborn, N.D., Luinge, W., et al. 2008, in: Proceedings of the Ninteenth International Symposium on Space Terahertz Technology, held in Groningen, Ed. Wolfgang Wild. p. 132
Tolls, V., Melnick, G.J., Ashby, L.M.N. et al. 2004, ApJSS 152, 137

[1] SRON Netherlands Institute for Space Research, Landleven 12, 9747 AD Groningen, the Netherlands
e-mail: p.r.roelfsema@sron.nl
[2] European Space Astronomy Centre, ESA, P.O. Box 78, E-28691 Villanueva de la Cañada, Madrid, Spain
[3] KOSMA, I.Physik.Institut, Universität zu Köln, Zülpicher Str. 77, 50937 Köln, Germany
[4] NHSC, California Institute of Technology, Pasadena, California, USA
[5] Chalmers University of Technology, SE-412 96 Göteborg, Sweden
[6] Max-Planck-Institut für Radioastronomie, Auf dem Hügel 69, D53121 Bonn, Germany
[7] Université de Toulouse, UPS-OMP, IRAP, Toulouse, France
[8] CNRS, IRAP, 9 Av. colonel Roche, BP 44346, F-31028 Toulouse Cedex 4, France
[9] Max-Planck Institute für Sonnensystemforschung, D-37191 Katlenburg-Lindau, Germany
[10] Laboratoire d'Etudes du Rayonnement et de la Matière en Astrophysique, UMR 8112 CNRS/INSU, OP, ENS, UPMC, UCP, Paris, France
[11] Osservatorio Astrofisico di Arcetri-INAF- Largo E. Fermi 5 I-50100 Florence, Italy
[12] Institute Fisica Spazio Interplanetario INAF, Via Fosso del Cavaliere 100, I-00133 Roma, Italy
[13] Department of Astronomy, Stockholm University, SE-106 91 Stockholm, Sweden
[14] Observatorio Astronómico Nacional (IGN), Centro Astronómico de Yebes, Apartado 148. 19080 Guadalajara, Spain
[15] Astronomical Institute, ETH, Zürich, 8093, Zürich, Switzerland
[16] Centro de Astrobiología (INTA-CSIC), Ctra de Torrejón a Ajalvir, km 4, 28850 Torrejón de Ardoz, Madrid, Spain
[17] Department of Physics & Astronomy, University of Waterloo, Waterloo, ON Canada N2L 3G1
[18] Joint Alma Observatory, Santiago, Chile
[19] Leiden Observatory, Leiden University, PO Box 9513, 2300 RA, Leiden, The Netherlands
[20] Physics Department, California Institute of Technology, Pasadena, California, USA
[21] Space Research Centre of the Polish Academy of Sciences, Bartycka 18A, 00-716 Warsaw, Poland
[22] Dept. of Experimental Physics, National University of Ireland, Maynooth, Co. Kildare, Ireland

[23] Université de Bordeaux, Observatoire Aquitain des Sciences de l'Univers, 2 rue de l'Observatoire, B.P.89, 33 271 Floirac Cedex, France

[24] CNRS, UMR 5804, Laboratoire d'Astrophysique de Bordeaux, 2 rue de l'Observatoire, B.P.89, 33 271 Floirac Cedex, France

[25] National Observatory of Athens, Greece

[26] Jet Propulsion Laboratories, Pasadena, California, USA

[27] LERMA-LRA, UMR 8112 du CNRS, Observatoire de Paris, École Normale Supérieure, UPMC & UCP, rue Lhomond, 75231 Paris Cedex 05, France

[28] Kapteyn Astronomical Institute, Landleven 12, 9747 AD Groningen, The Netherlands

[29] Department of Physics and Astronomy, Institute for Astronomy, KU Leuven, Celestijnenlaan 200D, 3001 Leuven, Belgium

[30] Department of Astronomy, University of Michigan, 500 Church Street, Ann Arbor, MI, 48109, USA

[31] UJF-Grenoble, CNRS-INSU, Institut de Planétologie et dAstrophysique de Grenoble (IPAG) UMR 5274, Grenoble, F-38041, France

[32] Astronomical Institute "Anton Pannekoek", University of Amsterdam, Science Park XH, Amsterdam, The Netherlands

[33] Nicolaus Copernicus Astronomical Center, Polish Academy of Sciences, ul Rabiańska 8, 87-100 Torún, Poland